

## On the Mechanism of Amiloride-Sensitive Nonelectrogenic $\text{Na}^+ - \text{H}^+$ Exchange in Cell Membranes: $\text{Na}^+/\text{H}^+$ Antiport or $\text{Na}^+/\text{OH}^-$ Symport?

V. S. MARKIN

*Frumkin Institute of Electrochemistry, Academy of Sciences of the USSR, Leninsky pr. 31, 117071 Moscow, USSR*

**Abstract.** The amiloride-sensitive and nonelectrogenic  $\text{Na}^+ - \text{H}^+$  exchange system of eucaryotic cells is currently a topic of great interest. The results of membrane transport in the presence of protons are shown to be similar in two cases: when  $\text{H}^+$  is transferred in one direction or  $\text{OH}^-$  — in the opposite direction. Therefore, in principle  $\text{Na}^+ - \text{H}^+$  exchange can be performed by two different mechanisms:  $\text{Na}^+/\text{H}^+$  antiport or  $\text{Na}^+/\text{OH}^-$  symport. However, the kinetic properties of these mechanisms turn out to be quite different. The present study analyses the simplest models of antiport and symport and delineates their important differences. For this purpose the Lineweaver-Burk plot presented as  $\text{Na}^+$  reverse flow entering a cell  $1/J_{\text{Na}}$  (or  $\text{H}^+$  leaving a cell) versus the reverse concentration of  $\text{Na}^+$  outside  $1/[\text{Na}^+]_0$  is most useful. If a series of lines with external pH as a parameter have a common point of intersection placed on the ordinate, it indicates the availability of  $\text{Na}^+/\text{H}^+$  antiport. In case of  $\text{Na}^+/\text{OH}^-$  symport a point of intersection is shifted to the left of the ordinate axis. According to data available in the literature,  $\text{Na}^+/\text{H}^+$  antiport manifests itself in dog kidney cells and in hamster lung fibroblasts. In the skeletal muscles of chicken and in rat thymus lymphocytes however, a  $\text{Na}^+/\text{OH}^-$  symport is apparently present.

### Introduction

Among various types of ion transport through cell membranes and cell organelles the  $\text{Na}^+ - \text{H}^+$  transfer and exchange are of primary importance (Krulwich 1983).  $\text{Na}^+ - \text{H}^+$  exchange is believed to provide a major mechanism for the removal of excess  $\text{Na}^+$  from the intracellular compartment in maintaining pH homeostasis (Nuccitelli and Deamer 1982); in the control of cell volume (Cala 1980); in the energy (ion gradients) accumulation in a cell (Skulachev 1978; Drachev et al. 1984); and in providing a means for the  $\text{Na}^+$ -coupled transfer of various metabolites (Saktor 1977; Jung et al. 1984).

In procaryotes  $\text{Na}^+ - \text{H}^+$  exchange can be both electroneutral and electrogenic. In eucaryotes  $\text{Na}^+ - \text{H}^+$  exchange is shown to be electroneutral and sensitive to the diuretic compound amiloride (Benos 1982). In recent years it became possible to study the kinetics of  $\text{Na}^+ - \text{H}^+$  exchange in more detail using this diuretic. Later, another and more active substance was identified — ethylisopropylamiloride — with a one hundred-fold greater potency than that of its precursor (Vigne et al. 1983).

Investigating the mechanism of  $\text{Na}^+ - \text{H}^+$  exchange, one finds that proton transfer from one solution to another is equivalent to  $\text{OH}^-$  transfer in the opposite direction. This process is also favoured by the high permeability of cell membranes to water molecules. Hence,  $\text{Na}^+ - \text{H}^+$  exchange can possibly take place by virtue of the mechanisms of both  $\text{Na}^+/\text{H}^+$  antiport and  $\text{Na}^+/\text{OH}^-$  symport. Usually researchers in this field do not attempt to distinguish between the two mechanisms and call them both as  $\text{Na}^+ - \text{H}^+$  exchange or  $\text{Na}^+/\text{H}^+$  antiport. For example, Krulwich's review begins: " $\text{Na}^+/\text{H}^+$  antiporter is a carrier which catalyzes  $\text{Na}^+ - \text{H}^+$  exchange, i. e. transfers  $\text{Na}^+$  and  $\text{H}^+$  through the membrane in the opposite directions or  $\text{Na}^+$  and  $\text{OH}^-$  in the same direction" (Krulwich 1983).

Such an approach is valid to some extent if one considers just **the result** of this exchange. But to study **the mechanism** of the process it is necessary to determine initially which particles are transferred. The exhaustive answer to this question can obviously be obtained only at the molecular level. However, the study of proteins responsible for this ion exchange was initiated only recently (Martin et al. 1984), and the only available information on the exchange mechanism is derived from the dependence of ion fluxes on the intracellular and extracellular concentration of transported ions.

It should be generally noted that researchers have often faced the problem of distinguishing the membrane transport of protons in one direction from that of hydroxides — in another. Furthermore it is evident that the problem can be successfully solved in artificial systems if appropriate experiments are carried out (Lieberman et al. 1983).

The present work is directed to the analysis of criteria that may help to distinguish  $\text{Na}^+/\text{H}^+$  antiport from  $\text{Na}^+/\text{OH}^-$  symport. In fact it is quite possible to distinguish between them if the kinetics of exchange are investigated. The present study concerns the most widely studied amiloride-sensitive nonelectrogenic  $\text{Na}^+ - \text{H}^+$  exchange in eucaryotic cells.

### Experimental data of primary importance

The kinetics of cation exchange are usually studied with vesicles from plasmatic membrane or directly with cultured cells. The data considered here were ob-

tained in numerous investigations: with chicken skeletal muscle (Vigne et al. 1982); rat thymus lymphocytes (Grinstein et al. 1984); membrane vesicles from renal brush border (Ives et al. 1983); dog kidney cells (Rindler and Saier 1981); and hamster lung fibroblasts (Paris and Pouyssegur 1983).

Cation transfer through the cellular membrane is observed by using: 1)  $^{22}\text{Na}$  in two ways — controlling its accumulation in the intracellular compartment or release into the extracellular medium; 2) by special probes — indicators of intracellular pH. In the last case it is possible to observe proton flow through the membrane.

The concentration dependence of such flows is studied by controlling changes in  $\text{Na}^+$  or  $\text{H}^+$  concentration.

In such experiments it was shown that the amiloride-sensitive  $\text{Na}^+ - \text{H}^+$  membrane exchanger was capable of the reversible transfer of these ions in both direction; the transfer stoichiometry was 1:1; the flows were saturable and were often described by Michaelis-Menten kinetics, particularly when studying  $\text{Na}^+$  entry into a  $\text{Na}^+$ -depleted cell. In this case  $\text{Na}_0^+ - \text{H}_i^+$  exchange occurs; where  $\text{Na}$  influx rises with increases in extracellular  $\text{Na}_0^+$  concentration and reaches saturation according to the Michaelis-Menten equation. Hydrogen ions present in the outer media serve as inhibitors of  $\text{Na}^+$  transfer into a cell.

The exchange system in question can transfer lithium instead of sodium but no affinity of the system for  $\text{K}^+$ ,  $\text{Cs}^+$  and  $\text{Rb}^+$  is shown. Lithium has some specific properties but its main transfer properties are similar to those of  $\text{Na}^+$  (Ives et al. 1983).

Due to the Michaelis-Menten properties of exchange it is possible to analyse the flows by the methods of enzyme kinetics. The optimal method of graphical analysis is that whereby coordinates present the flow concentration dependencies as straight lines. The axis intercepts can indicate the important transfer features of the system. The Lineweaver-Burk plot is most popular: where the inverse flow (e. g.,  $1/J_{\text{Na}}$ ) is plotted against the inverse concentration of transferred ion ( $1/[\text{Na}_0^+]$ ). In the above-studies kinetic curve shown to be linear using the Lineweaver-Burk plot (see Fig. 1).

Changes in line positions with a change in extracellular concentration of protons  $[\text{H}^+]_0$  are of particular interest. Usually a few dependencies corresponding to different  $\text{pH}_0$  values are experimentally obtained and a decrease in  $\text{pH}_0$  causes the slope of the line to be greater. It is a remarkable feature of the Lineweaver-Burk plot that all its lines have a common point of intersection. As shown below, the position of this point on the plot is very informative for it describes an important quantitative as well as qualitative characteristic of the ion transfer mechanism.

As protons in the outer medium suppress sodium transfer into cell the Dixon plot is often used on the coordinates  $1/J_{\text{Na}} - [\text{H}^+]_0$  to analyse the flow depen-

dence on external concentration of  $H_0^+$ . This presentation is designed for studying inhibitor effects because, as known from enzymic kinetics, the curves become linear in this case. In fact, the concentration dependence of the reverse flow is actually presented by a straight line (see Fig. 2a).

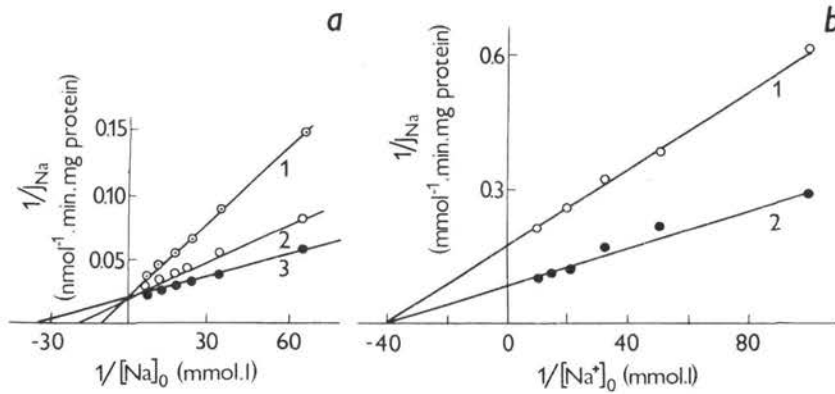


**Fig. 1.**  $Na^+$  influx versus  $Na^+$  extracellular concentration in the Lineweaver-Burk plot. Extracellular pH values are given in the graphs. *a*)  $Na^+$  - depleted kidney cells of dog. Experimental points are from Rindler and Saier (1981). Lines are plotted using formula (7). 1 -  $pH_0 = 6$ , 2 -  $pH_0 = 7.5$ , 3 -  $pH_0 = 9$ . *b*)  $Na^+$  - depleted skeletal muscle of chicken. Experimental points are from Vigne et al. (1982). Lines are plotted using formula (10). 1 -  $pH_0 = 7.5$ , 2 -  $pH_0 = 8.5$ .

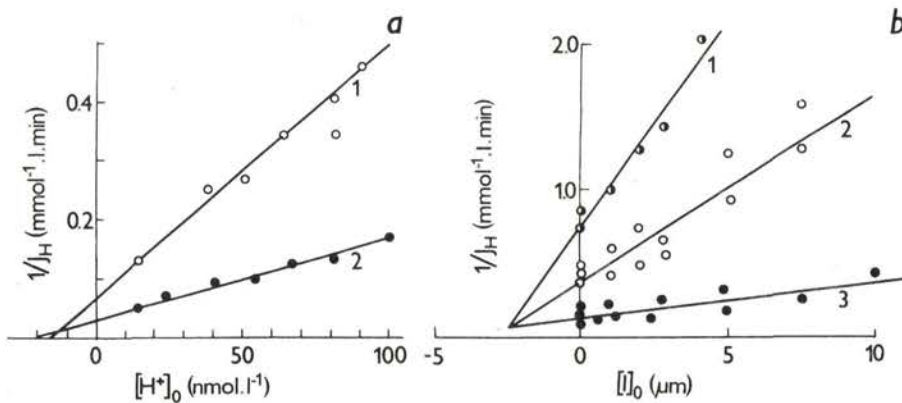


**Fig. 2.** Dixon plot for proton efflux versus extracellular concentration of protons (*a*) and amiloride (*b*). External concentration of  $Na^+$  ions is given in the plots. Experimental points for rat thymus lymphocytes are from Grinstein et al. (1984). Lines are plotted using equation (19). *a*: 1 -  $[Na^+]_0 = 20 \text{ mmol} \cdot \text{l}^{-1}$ , 2 -  $70 \text{ mmol} \cdot \text{l}^{-1}$ . *b*: 1 -  $[Na^+]_0 = 10 \text{ mmol} \cdot \text{l}^{-1}$ , 2 -  $20 \text{ mmol} \cdot \text{l}^{-1}$ , 3 -  $70 \text{ mmol} \cdot \text{l}^{-1}$ .

The Dixon plot is also used to describe the amiloride effect (see Fig. 2*b*) in relation to the dependence  $1/J_{\text{Na}} - [I]_0$ . The Eadie-Hofstee plot is, however, sometimes used with the coordinates  $J_{\text{Na}} - J_{\text{Na}}/[I]_0$  when a series of curves is plotted with the inhibitor concentration  $[I]_0$  serving as a parameter. Here a family of lines is also obtained (see Fig. 3) and the point of intersection is once again of interest.

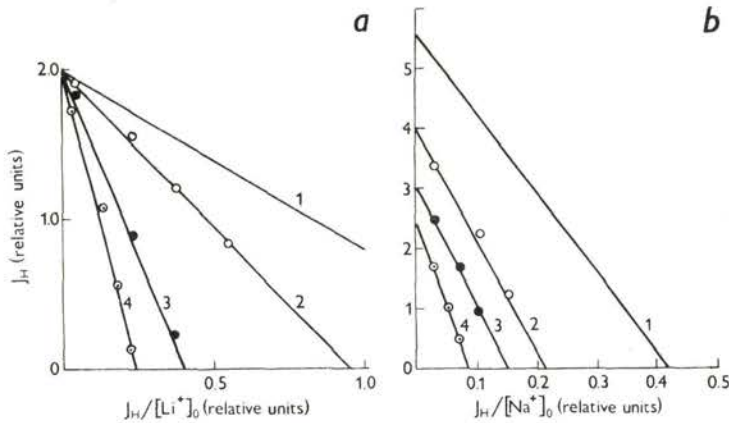


**Fig. 3.** Effects of amiloride on proton efflux from renal brush border vesicles. Amiloride concentration is shown on the curves. Proton efflux is stimulated by external addition of lithium (*a*) and sodium (*b*). Experimental points are from Ives et al. (1983). Lines are plotted using equations (7) and (19) with  $\text{H}^+$  extracellular ions serving as amiloride. Amiloride concentrations ( $\mu\text{mol} \cdot \text{l}^{-1}$ ): 1 - 0, 2 - 25, 3 - 50, 4 - 100.

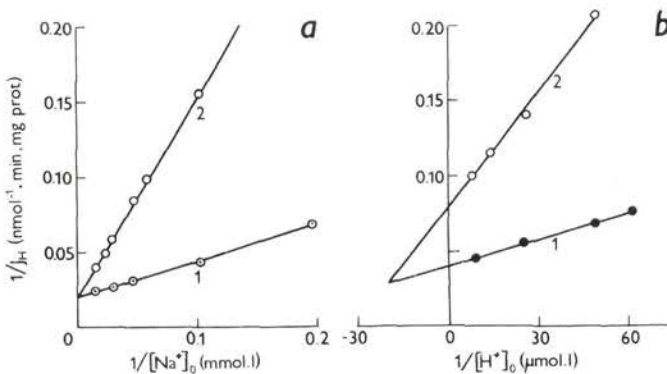


**Fig. 4.** Effect of amiloride on exchange flows in lung fibroblasts of hamster. Amiloride concentration is shown on the curves. *a*) Dependence of proton efflux on the extracellular concentration of  $\text{Na}^+$ . Amiloride concentrations ( $\mu\text{mol} \cdot \text{l}^{-1}$ ): 1 - 0, 2 - 5. *b*) Dependence of proton influx on external concentration of protons. Cells are loaded with lithium and placed in  $\text{Na}^+$  - free medium. Experimental points are from Paris and Pouyssegur (1983). Lines are plotted using equations (7) and (19). Amiloride concentrations ( $\mu\text{mol} \cdot \text{l}^{-1}$ ): 1 - 0, 2 - 10.

Finally, the Lineweaver-Burk plot can be also used to analyse the amiloride effect with amiloride concentration as a parameter (see Fig. 4).

Using these plots, important parameters of ion transfer can be determined, in particular, the maximum flow values and the Michaelis constants. There is, however, only some formal similarity between the enzymic kinetics and the ion transfer through membranes. And though this form of analysis can be useful for analysing ion competitive interaction on the same side, it is quite difficult to apply on the opposite sides. It is, therefore, necessary to apply mathematic models specially developed for the description of membrane transport.

### $\text{Na}^+/\text{H}^+$ antiport model

In the models of facilitated membrane transport either channels or carriers present in the membrane are generally considered. The carrier models include not only the most simple mobile carrier of the valinomycin type, but also more complex constructions, e.g. rotating and oscillating protein globules which expose their "transport site" to each side of membrane as a result of such rotation. Transfer by means of carriers is of a cycle character and is apparently best suited for mediating exchange processes due to its physical nature. Carrier-transport is, therefore, considered in depth in the present study.

To describe coupled transport a number of carrier models capable of binding various ions have been proposed (Wilbrandt 1972; Heinz et al. 1972; Markin and Chizmadzhev 1974).

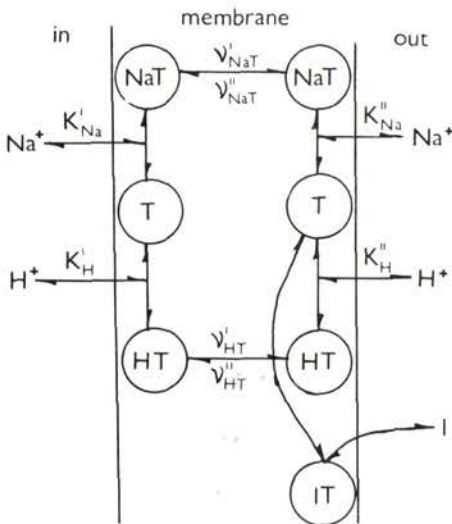


**Fig. 5.** Model of  $\text{Na}^+/\text{H}^+$  antiport. Competitive inhibitor I is in the external solution.

Beginning with Na<sup>+</sup>/H<sup>+</sup> antiport, let us assume that there is a carrier (T) in the membrane which can be competitively bound to Na<sup>+</sup> and H<sup>+</sup> ions from the surrounding solutions (see Fig. 5). Alongside the free form of carrier T this may result in the presence of the loaded forms of NaT and HT in the membrane. The transition from the free to the loaded form occurs at the membrane boundary with equilibrium constants of the corresponding reaction designated as K'\_{Na} and K'\_H on the inner side of the membrane and K''\_{Na} and K''\_H — on the outer side. Thus, the equilibrium between [Na<sup>+</sup>] and [H<sup>+</sup>] concentrations in solution and those of various carrier forms [T]<sub>i</sub>, [NaT]<sub>i</sub> and [HT]<sub>i</sub> at the left boundary inside the membrane are determined by the following ratios:

$$\begin{aligned} [\text{Na}^+]_i [\text{T}]_i &= K'_{\text{Na}} [\text{NaT}]_i \\ [\text{H}^+]_i [\text{T}]_i &= K'_H [\text{HT}]_i \end{aligned} \quad (1)$$

The equivalent ratios for the right boundary are:

$$\begin{aligned} [\text{Na}^+]_0 [\text{T}]_0 &= K''_{\text{Na}} [\text{NaT}]_0 \\ [\text{H}^+]_0 [\text{T}]_0 &= K''_H [\text{HT}]_0 \end{aligned} \quad (2)$$

The further introduction of reduced ion concentration is thought to be expedient:

$$\begin{aligned} [\tilde{\text{Na}}^+]_i &= [\text{Na}^+]_i / K'_{\text{Na}} & [\tilde{\text{H}}^+]_i &= [\text{H}^+]_i / K'_H \\ [\tilde{\text{Na}}^+]_0 &= [\text{Na}^+]_0 / K''_{\text{Na}} & [\tilde{\text{H}}^+]_0 &= [\text{H}^+]_0 / K''_H \end{aligned} \quad (3)$$

The loaded carrier forms NaT and HT can penetrate the membrane. Let us designate the left-to-right transfer rates as  $v'_{\text{NaT}}$  and  $v'_{\text{HT}}$  and right-to-left ones as  $v''_{\text{NaT}}$  and  $v''_{\text{HT}}$ . In general the free carrier form can also penetrate the membrane but in such a case there will be no complete coupling of ion fluxes and the exchange stoichiometry will be variable (Markin and Chizmadzev 1974). As constant stoichiometry of exchange (1:1) is under consideration we assume that the free carrier does not move through the membrane.

Calculation of this model results in estimation of Na<sup>+</sup> ion influx entering a cell:

$$\begin{aligned} J_{\text{Na}} &= (v'_{\text{HT}} v''_{\text{NaT}} [\tilde{\text{H}}^+]_i [\text{Na}^+]_0 - v''_{\text{HT}} v'_{\text{NaT}} [\tilde{\text{H}}^+]_0 [\tilde{\text{Na}}^+]_i) \times \\ &\times \{ (1 + [\tilde{\text{H}}^+]_i + [\tilde{\text{Na}}^+]_i) (v'_{\text{HT}} [\tilde{\text{H}}^+]_0 + v''_{\text{NaT}} [\tilde{\text{Na}}^+]_0) + \\ &+ (1 + [\tilde{\text{H}}^+]_0 + [\tilde{\text{Na}}^+]_0) (v'_{\text{HT}} [\tilde{\text{H}}^+]_i + v''_{\text{NaT}} [\tilde{\text{Na}}^+]_i) \}^{-1} \end{aligned} \quad (4)$$

The equation for flux per molecule of carrier is presented.

Due to the passive character of ion exchange the transfer should stop in the absence of concentration gradients.

This indicates the relation between the transfer rate constants:

$$\frac{v'_{HT}K''_H}{v''_{HT}K'_H} = \frac{v'_{NaT}K''_{Na}}{v''_{NaT}K'_{Na}} \quad (5)$$

The flow is usually considered as a function of two variables, e. g. external concentrations  $[Na^+]_0$  and  $[H^+]_0$ . First, we consider the dependence of flow on concentration  $[Na^+]_0$ .

If the Lineweaver-Burk plot is prepared using equation (4) it can be clearly seen that no linearization of curves occurs due to the presence of  $v'_{HT}v'_{NaT}[\tilde{H}^+]_i[\tilde{Na}^+]_i$  in the numerator of equation (4). However, in experiments with  $Na^+$ -depleted cells this term can be neglected.

The maximum flow is designated:

$$J_{Na}^{max} = \frac{v'_{HT}v'_{NaT}[\tilde{H}^+]_i}{v''_{NaT} + (v'_{HT} + v''_{NaT})[\tilde{H}^+]_i} \quad (6)$$

then from equation (4):

$$\frac{J_{Na}^{max}}{J_{Na}} = 1 + \frac{v'_{HT}[\tilde{H}^+]_i + (v'_{HT}[\tilde{H}^+]_i + v'_{HT}(1 + [\tilde{H}^+]_i))[\tilde{H}^+]_0}{(v''_{NaT} + (v'_{HT} + v''_{NaT})[\tilde{H}^+]_i)[\tilde{Na}^+]_0} \quad (7)$$

It is clearly seen that on the Lineweaver-Burk plot this dependence will be presented as a straight line (see Fig. 6a). The increased parameter  $[H^+]_0$  causes the slopes of lines to be greater, indicating a decrease in the flow. It is very important that all lines have a common point of intersection at the ordinate axis, corresponding to maximum flow  $J_{Na}^{max}$ .

The line with the least slope corresponds to a zero external concentration of protons making the intercept  $-1/K_m$  at the abscissa where  $K_m$  can be referred to as the Michaelis constant.

$$K_m = \frac{v'_H[\tilde{H}^+]_i K''_{Na}}{v''_H + (v'_H + v''_H)[\tilde{H}^+]_i} \quad (8)$$

The intersections produced by other lines can be also referred to as Michaelis constants corresponding to the given concentration  $[H^+]_0$ . Such values are called apparent constants ( $K_{m,app}$ ).

The Dixon plot with a dependence of  $1/J_{Na}$  on  $[H^+]_0$  (see Fig. 6b) has also a series of lines with the concentration  $[Na^+]_0$  as a parameter. All lines have a common point of intersection with coordinates  $(-H_D$  and  $1/J_{Na}^{max})$ .

$$H_D = \frac{v'_H[\tilde{H}^+]_i K'_H}{v''_H + (v'_H + v''_H)[\tilde{H}^+]_i} \quad (9)$$

It should be noted that the horizontal line corresponds to high concentration of Na.

The Eadie-Hofstee plot for the flow  $J_{\text{Na}}$  as a function of  $J_{\text{Na}}/[\text{Na}^+]_0$  with proton concentration  $[\text{H}^+]_0$  as a parameter is shown in Fig. 6c. The lines have a common point of intersection which is placed on the y-axis and indicates the maximum possible value of flow. This is the typical Eadie-Hofstee plot for a

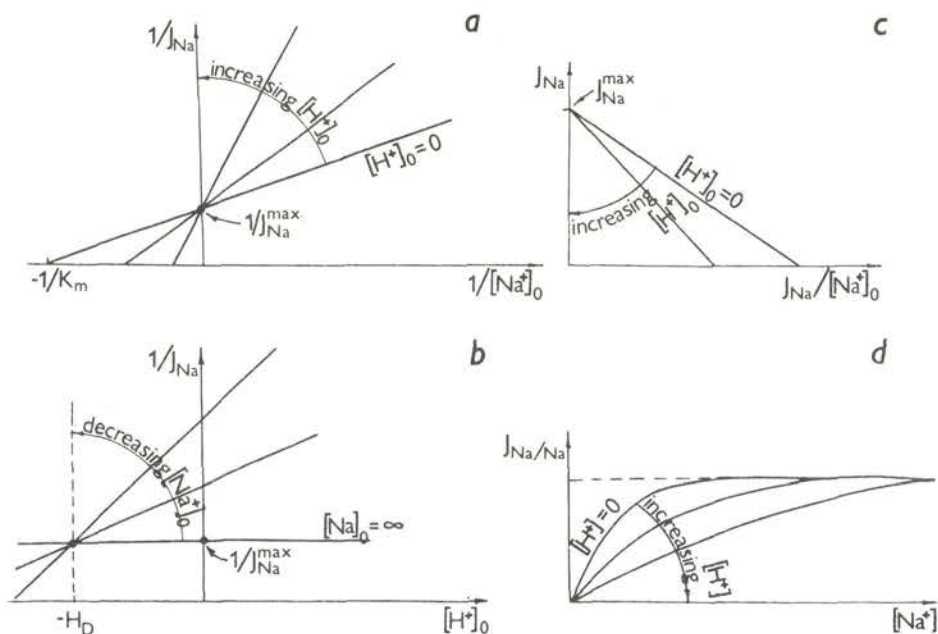


**Fig. 6.** Concentration dependence of exchange flows in the  $\text{Na}^+/\text{H}^+$  antiport model with a  $\text{Na}^+$ -depleted cell. *a*) the Lineweaver-Burk plot, *b*) Dixon plot, *c*) the Eadie-Hofstee plot, *d*)  $\text{Na}^+/\text{Na}^+$  exchange under symmetrical conditions versus  $\text{Na}^+$  concentration.

competitive inhibitor in enzymic catalysis (Segel 1975).

The exchange of similar ions ( $\text{Na}^+/\text{Na}^+$  exchange) is of considerable interest. To separate this homoexchange from other flows, this exchange is usually studied at similar concentrations on both sides of a membrane. The exchange occurs due to unilateral flows with the resultant Na flow being equal to zero. If the membrane is assumed to be symmetrical then  $\text{Na}^+/\text{Na}^+$  exchange is described as follows:

$$J_{\text{Na}/\text{Na}} = \frac{v_{\text{NaT}}[\tilde{\text{Na}}^+]}{2(1 + [\tilde{\text{H}}^+] + [\tilde{\text{Na}}^+])} \quad (10)$$

Fig. 6*d* shows the plot of this dependence with proton concentration as a curve parameter. It can be seen that all functions gradually increase, each at its own rate, reaching one and the same threshold.

Finally, we consider the effect of amiloride (1) on ion exchange. Assuming that amiloride competes with  $\text{Na}^+$  and  $\text{H}^+$  ions for a binding site on the outer side of membranes, thus immobilizing a carrier: the compound IT will appear on the outer side of the membrane (Fig. 5*b*) together with the compounds mentioned above (see Fig. 5*a*). Considering the equations, it can be seen that the amiloride effect on  $\text{Na}^+$  influx is similar to that of extracellular  $\text{H}^+$  ions with kinetic curves as shown in Figs. 6*b* and 6*d*.

### Model of $\text{Na}^+/\text{OH}^-$ symport

Let us consider another possibility assuming that the carrier T has two binding sites: one for  $\text{Na}^+$  and another for  $\text{OH}^-$  (see Fig. 7). Then the compounds T, NaT, TOH and NaTOH can be simultaneously present in the membrane with an equilibrium between them and  $\text{Na}^+$  and  $\text{OH}^-$  ions respectively on the inner side of the membrane:

$$\begin{aligned} [\text{Na}^+]_i[\text{T}]_i &= K'_{\text{Na}}[\text{NaT}]_i \\ [\text{OH}^-]_i[\text{T}]_i &= K'_{\text{OH}}[\text{TOH}]_i \\ [\text{Na}^+]_i[\text{OH}^-]_i[\text{T}]_i &= K'_{\text{NaTOH}}[\text{NaTOH}]_i \end{aligned} \quad (11)$$

Similar equations can be presented for the outer side of the membrane with equilibrium constants being marked by two primes.

Such a ratio of equilibrium constants represented as:

$$\lambda' = K'_{\text{Na}}K'_{\text{OH}}/K'_{\text{NaTOH}} \quad (12)$$

indicates the ternary complex stability or the strength of  $\text{Na}^+$  and  $\text{OH}^-$  in binding with the carrier T. If  $\lambda' > 1$ , there is mutual attraction between these ligands, and if  $\lambda' < 1$ , there is repulsion.  $\lambda''$  — is a similar parameter for the outer side of the membrane.

Introducing reduced variables:

$$[\tilde{\text{Na}}^+]_i = [\text{Na}^+]_i/K'_{\text{Na}} \text{ and } [\tilde{\text{OH}}^-]_i = [\text{OH}^-]_i/K'_{\text{OH}} \quad (13)$$

we obtain

$$\begin{aligned} [\tilde{\text{Na}}^+]_i[\text{T}]_i &= [\text{NaT}]_i; \quad [\tilde{\text{OH}}^-]_i[\text{T}]_i = [\text{TOH}]_i \\ \lambda'[\tilde{\text{Na}}^+]_i[\tilde{\text{OH}}^-]_i[\text{T}]_i &= [\text{NaTOH}]_i \end{aligned} \quad (14)$$

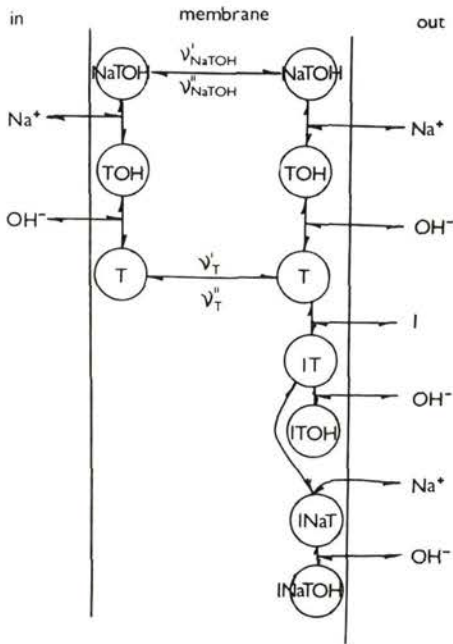


Fig. 7. Model of  $\text{Na}^+/\text{OH}^-$  symport. Inhibitor I is in the outer medium.

Unlike the binary complexes  $\text{NaT}$  and  $\text{TOH}$  the free carrier  $\text{T}$  and ternary complex  $\text{NaTOH}$  are presumably capable of moving through the membrane. Rate constants of transfer from one side of the membrane to another:

$$v'_T, v''_T, v'_{\text{NaTOH}} \text{ and } v''_{\text{NaTOH}}$$

As in the antiport model, there should be a relation between rate constants:

$$\frac{v'_T v''_{\text{NaTOH}} \lambda''}{K''_{\text{Na}} K''_{\text{OH}}} = \frac{v'_T v'_{\text{NaTOH}} \lambda'}{K'_{\text{Na}} K'_{\text{OH}}} \quad (15)$$

Calculation of this model results in the estimation of  $\text{Na}$  influx:

$$\begin{aligned} J_{\text{Na}} = & (\lambda'' v'_T v''_{\text{NaTOH}} [\tilde{\text{Na}}^+]_0 [\tilde{\text{OH}}^-]_0 - \lambda' v'_T v'_{\text{NaTOH}} [\tilde{\text{Na}}^+]_i [\tilde{\text{OH}}^-]_i) \times \\ & \times (1 + [\tilde{\text{Na}}^+]_i + [\tilde{\text{OH}}^-]_i + \lambda' [\tilde{\text{Na}}^+]_i [\tilde{\text{OH}}^-]_i) (v'_T + \\ & + \lambda'' v''_{\text{NaTOH}} [\tilde{\text{Na}}^+]_0 [\tilde{\text{OH}}^-]_0) + (1 + [\tilde{\text{Na}}^+]_0 + [\tilde{\text{OH}}^-]_0 + \\ & + \lambda' [\tilde{\text{Na}}^+]_0 [\tilde{\text{OH}}^-]_0) (v'_T + \lambda' v'_{\text{NaTOH}} [\tilde{\text{Na}}^+]_i [\tilde{\text{OH}}^-]_i)^{-1} \end{aligned} \quad (16)$$

Such a dependence can be shown as a linear pattern if any ion is absent on

one side of the membrane. Let  $[\text{Na}^+]_0 = 0$ . The maximum possible value of flow at very high concentrations  $[\text{Na}^+]_0$  and  $[\text{OH}^-]_0$  is represented as:

$$J_{\text{Na}}^{\text{max}} = \frac{v'_T v''_{\text{NaTOH}}}{v'_T + v''_T(1 + [\widetilde{\text{OH}}^-]_i)} \quad (17)$$

Concentrations of hydrogen and hydroxyl ions are related in the solution:

$$[\text{H}^+]_0[\text{OH}^-]_0 = K_w \quad (18)$$

where  $K_w$  represents the ion product of water equal to  $1 \times 10^{-14} \text{M}^2$ .

Then  $\text{Na}^+$  influx can be presented in another way:

$$\frac{J_{\text{Na}}^{\text{max}}}{J_{\text{Na}}} = 1 + \frac{v'_T}{\lambda''(v'_T + v''_{\text{NaTOH}}(1 + [\widetilde{\text{OH}}^-]_i))} \times \left\{ \frac{K''_{\text{OH}}[\text{H}^+]_0}{K_w} + \frac{1}{[\widetilde{\text{Na}}^+]_0} + \frac{1 + (v''_T/v'_T)(1 + [\widetilde{\text{OH}}^-]_i)}{[\widetilde{\text{Na}}^+]_0} \times \frac{K''_{\text{OH}}[\text{H}^+]_0}{K_w} \right\} \quad (19)$$

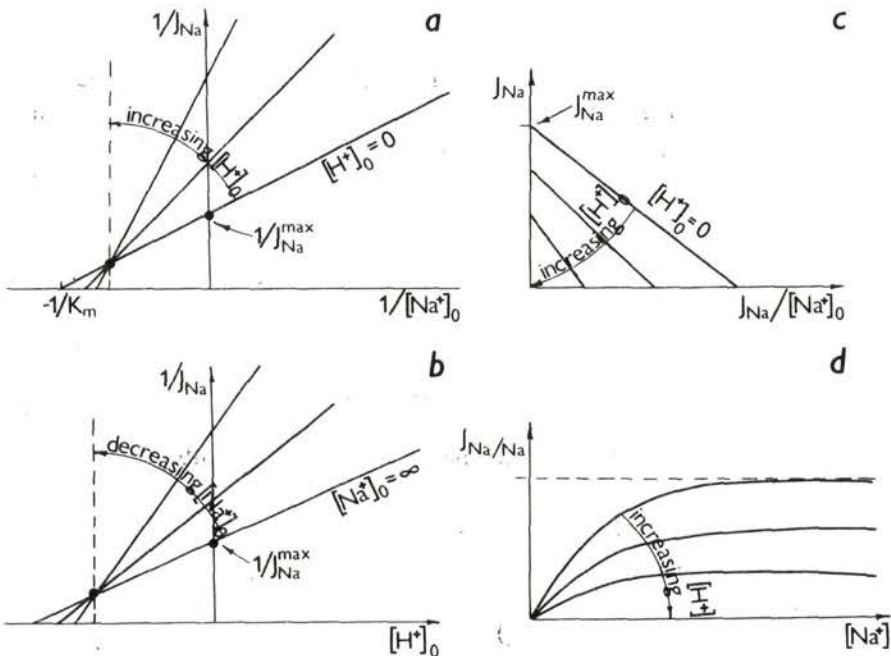


**Fig. 8.** Concentration dependence of  $\text{Na}^+$  flow in the model of  $\text{Na}^+/\text{OH}^-$  symport with a  $\text{Na}^+$ -depleted cell. *a)* the Lineweaver-Burk plot, *b)* Dixon plot, *c)* the Eadie-Hofstee plot, *d)*  $\text{Na}^+/\text{Na}^+$  exchange rate versus  $\text{Na}^+$  concentration under symmetrical conditions.

On the Lineweaver-Burk plot (Fig. 8a) a series of lines is shown with the slope increasing with an increase in  $[\text{H}^+]_0$ . All lines have a common point of intersection with coordinates:

$$-\frac{1}{K''_{\text{Na}}(1 + (v''_{\text{T}}/v_{\text{T}})(1 + [\widetilde{\text{OH}}^-]_i))} \quad \text{at the abscissa (20)}$$

and

$$\frac{1}{J_{\text{Na}}^{\text{max}}} \left\{ 1 - \frac{1}{\lambda'' \left( 1 + \frac{v''_{\text{NaTOH}}}{v_{\text{T}}} (1 + [\text{OH}^-]_i) \right) \left( 1 + \frac{v''_{\text{T}}}{v_{\text{T}}} (1 + [\widetilde{\text{OH}}^-]_i) \right)} \right\} \quad \text{at the ordinate (21)}$$

As seen from equation (19) a point of intersection of all the lines can be above and below the abscissa depending on the summand values inside the parentheses. Everything is determined by the following value:

$$\lambda'' \left( 1 + \frac{v''_{\text{NaTOH}}}{v_{\text{T}}} (1 + [\widetilde{\text{OH}}^-]_i) \right) \left( 1 + \frac{v''_{\text{T}}}{v_{\text{T}}} (1 + [\widetilde{\text{OH}}^-]_i) \right) \quad (22)$$

If it is  $> 1$ , the intersection point is above the abscissa. As the value inside the parentheses is  $> 1$  a  $\lambda''$  value of  $\geq 1$  is sufficient for the net value of (22) to be  $> 1$ . Because the ligands  $\text{Na}^+$  and  $\text{OH}^-$  being bound to a carrier are oppositely charged, their synergetic interaction is therefore expected.

The intersection below the abscissa means  $\lambda'' < 1$ , i. e. on interaction with a carrier the ligands are mutually repelled.

Different lines of the series given in Fig. 6a yield different intercepts on the ordinate depending on the pH of the external solution. The line corresponding to  $[\text{H}^+]_0 = 0$  has the lowest point of intersection with the ordinate, and it is this intercept that determines the maximum flow value. Intersection of the same line with the abscissa determines the Michaelis constant:

$$K_{\text{m}} = \frac{K''_{\text{Na}}}{\lambda'' \left( 1 + \frac{v''_{\text{NaTOH}}}{v_{\text{T}}} (1 + [\widetilde{\text{OH}}^-]_i) \right)} \quad (23)$$

Lines with arbitrary pH values of external solution make the intercepts determining the apparent Michaelis constant:

$$K_{\text{m,app}} = K''_{\text{Na}} \cdot \frac{K_{\text{w}} + K''_{\text{OH}}[\text{H}^+]_0(1 + (1 + [\widetilde{\text{OH}}^-]_i)v''_{\text{T}}/v_{\text{T}}/v_{\text{T}})}{K''_{\text{OH}}[\text{H}^+]_0 + \lambda''_{\text{NaTOH}}(1 + (1 + [\widetilde{\text{OH}}^-]_i)v''_{\text{NaTOH}}/v_{\text{T}})} \quad (24)$$

The Dixon plot for  $1/J_{\text{Na}}$  as a function of  $[\text{H}^+]_0$  is shown in Fig. 8b with the  $[\text{Na}^+]_0$  parameter for a series of lines possessing a common point of intersection with coordinates

$$-\frac{K_w}{K''_{\text{OH}}(1 + (v''_T/v'_T) \cdot (1 + [\tilde{\text{O}}\text{H}^-]_i))} \text{ at the abscissa} \quad (25)$$

and

$$\frac{1}{J_{\text{Na}}^{\text{max}}} \left\{ 1 - \frac{1}{\lambda'' \left( 1 + \frac{v''_{\text{NaTOH}}}{v'_T} (1 + [\tilde{\text{O}}\text{H}^-]_i) \right) \left( 1 + \frac{v''_T}{v'_T} (1 + [\tilde{\text{O}}\text{H}^-]_i) \right)} \right\} \quad (26)$$

at the ordinate.

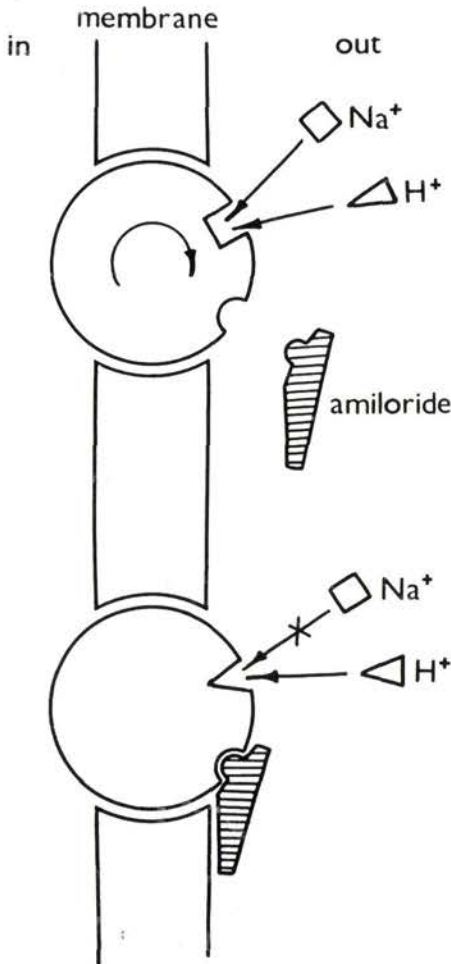


**Fig. 9.** A possible scheme of competitive  $\text{Na}^+/\text{H}^+$  antiport inhibition. In the absence of amiloride,  $\text{Na}^+$  and  $\text{H}^+$  ions compete for the transport site. Under amiloride binding on the control centre the transport site is distorted making  $\text{Na}^+$  binding impossible while  $\text{H}^+$  can be still bound.

The latter coincides with similar coordinates on the Lineweaver-Burk plot, therefore all the above considerations refer to it as well. Specifically, this plot can also be above or below the abscissa depending on the system parameters.

The Eadie-Hofstee plot for  $J_{\text{Na}}$  against  $J_{\text{Na}}/[\text{Na}^+]_0$  shows a family of lines, approaching the origin of coordinates with a rise in proton concentration  $[\text{H}^+]_0$ , but their slopes can both increase and decrease. The result is also dependent on value (22). If it is  $> 1$  the slope becomes greater with increases in  $[\text{H}^+]_0$  (see Fig. 8c) so that the lines converge in the left top section of the plot. In the opposite case, they converge in the right bottom section of the plot.

The lines have many points of intersection dispersed on the plot.

In conclusion we consider the possibility for  $\text{Na}^+/\text{Na}^+$  exchange. Assuming the concentration of compounds on both sides of membrane to be equal and the membrane to be symmetrical, the exchange flux is expressed as:

$$J_{\text{Na}/\text{Na}} = \frac{v_{\text{NaTOH}} [\tilde{\text{N}}_a^+] [\tilde{\text{O}}\text{H}^-]}{2(1 + \tilde{\text{N}}_a^+)(1 + [\tilde{\text{O}}\text{H}^-])} \quad (27)$$

Fig. 8d shows the plot of such a relation, with proton concentration being a parameter of the curves. It can be seen that the functions gradually increase and reach their threshold values corresponding to their pH.

Finally, let us consider the inhibition of symport by amiloride. Assume that amiloride has its own binding site so that any combination of adsorbed ligands can take place. To describe the relative stability of different complexes the corresponding coefficient ( $\lambda$ ) can be introduced. Similar calculations yield kinetic curves with the amiloride effect taken into account. The role of amiloride is shown to be similar to the interaction of  $[\text{Na}^+]_0$  and  $[\text{H}^+]_0$  ions.

## Discussion

Two models of coupled ion transfer have been considered and some features of their similarity and difference have been shown. In fact, both models are capable of  $\text{Na}^+ - \text{H}^+$  exchange but different mechanisms are involved.  $\text{Na}^+/\text{H}^+$  antiporter directly exchanges  $\text{Na}^+$  ions for protons and  $\text{Na}^+/\text{OH}^-$  symporter (together with Na) carries  $\text{OH}^-$  ion which interacts with  $\text{H}^+$  ions on the opposite side reducing their concentration. The final results are similar for both models.

The thermodynamic properties of both systems are essentially the same. Equations (4) and (16) show that in both models the system comes to equilibrium provided that

$$[\text{H}^+]_i/[\text{H}^+]_0 = [\text{Na}^+]_i/[\text{Na}^+]_0 \quad (28)$$

The kinetic properties, however, turn out to be quite different for the two models. This can be clearly seen on the Lineweaver-Burk and Eadie-Hofstee plots.

On the Lineweaver-Burk plot in case of antiport all lines have a common point of intersection on the ordinate and in case of symport this point is shifted to the left half-plane. Since the ordinate intercept indicates the value of maximum permissible flow at the given value of  $[H^+]_0$ , in case of antiport the maximum  $Na^+$  influx does not depend on the external proton concentration. It is quite a reasonable result, for in the usual case of competition for a binding site an increase in  $Na^+$  concentration finally leads to the loading of almost all carriers with  $Na^+$  at the outer membrane boundary. Consequently, the limiting flow should not be actually dependent on proton concentration in the outer medium.

By contrast, in case of  $Na^+/OH^-$  symport, the ion influx is determined by the number of ternary complexes ( $NaTOH$ ) in the membrane. Such a quantity is shown still to be dependent on  $[OH^-]_0$ , i.e. on  $[H^+]_0$ , even at a very high concentration of  $[Na^+]_0$ . As a result of this, the lines have different points of intersection with the ordinate.

Such a difference is also clearly seen on the Eadie-Hofstee plot (see Figs. 6c and 8c). In case of antiport the lines have a common point of intersection on the ordinate, and in case of symport no such intersection is shown and the lines converge in the left top section. The reason for this difference is as described above. Moreover, the difference can be even more apparent if the lines (see Fig. 6b) tend to converge in the right bottom section.

There is no apparent difference between the Dixon plots shown in Figs. 6b and 8b. In both cases the lines tend to converge at one and the same point. The only difference being that in the case of antiport the limiting line corresponding to very high  $Na^+$  concentration is horizontal. The convergence point is, therefore, at the level corresponding to the maximum possible flow. In case of symport this position is determined by a complex combination of system parameters so that under certain conditions it can be shifted to the bottom half plane.

Finally,  $Na^+/Na^+$  exchange was compared in both models. Under symmetrical conditions  $Na^+/Na^+$  exchange flows increase with rising  $Na^+$  concentrations, but in case of antiport the threshold values do not depend on the pH of surrounding solutions and in case of symport the thresholds vary at different pH values.

Thus, the study of exchange kinetics indicates that the Lineweaver-Burk plot is the most suitable means for distinguishing between the two models.

The process of  $Na^+-H^+$  exchange has been experimentally studied in a great number of systems, which exhibited similar properties: e.g. Michaelis constants for  $Na^+$  were 59 mmol/l in rat thymus lymphocytes (Grinstein et al.

1984); 6–7 mmol/l in renal microvillus membrane vesicles (Kinsella and Aronson 1980, 1981); 11.3 mmol/l in the gallbladder of amphibians (Weinman and Reuss 1982); and 25 mmol/l in the skeletal muscles (Bigne et al. 1982). Inhibitor effects are often similar as well, though the constants of inhibition can be quite different. However, some qualitative differences do exist as well. It is true that only few studies provide sufficient data for determining the mechanism of exchange. The data for two entirely different systems are shown in Figs. 1*a* and 1*b*. The Lineweaver-Burk plots obtained for dog kidney cells (Rindler and Saier 1981) have a common point of intersection on the ordinate (see Fig. 1*a*). Hence, the exchange of this system can be described by  $\text{Na}^+/\text{H}^+$  antiport. Similar results have been obtained for hamster lung fibroblasts (Paris and Pouyssegur 1983) to show the action of the  $\text{Na}^+/\text{H}^+$  antiporter.

On the contrary, in the chicken skeletal muscles (Vigne et al. 1982) the kinetic lines have a point of intersection located far to the left of the ordinate (see Fig. 1*b*). Such an exchange can be described by  $\text{Na}^+/\text{OH}^-$  symport. The same mechanism is apparently shown for rat thymus lymphocytes (Grinstein et al. 1984) though there is no representation of the necessary plot in this work. If the data of Grinstein et al. (1984), from Fig. 6*b* are however, represented as a Lineweaver-Burk plot the point of intersection will not be present on the ordinate. It should be noted that these authors included the words “ $\text{Na}^+/\text{H}^+$  antiport” in the title of their article but in the text they pointed out that the observed changes in  $\text{pH}_i$  could be accounted for not only by  $\text{H}^+$  release but also by  $\text{OH}^-$  accumulation. It seems that the words “ $\text{H}^+$  release” are used to simplify the presentation whereas  $\text{OH}^-$  accumulation is evident from their experimental data.

Thus, all data in the literature can be distributed between two possible models of coupled transport. It should be noted, however, that only two **most simple** models of transfer are considered in the present work and the mechanism describing the experimental data can be attributed to only one of these. These mechanisms present two extreme possibilities based on the entirely different suggestions. And the purpose of our analysis lies in disclosing the major differences of the most “pure” models.

The actual situation can obviously be more complex and cellular exchange can involve the properties of various models. For example, in the analysis of  $\text{Na}^+/\text{H}^+$  antiport we considered simple competition among exchange ions for a transfer site. But assuming that these ions have different binding sites the result will be also quite different.

In fact, there are some data indicating the existence of really complex properties of  $\text{Na}^+/\text{H}^+$  exchange. In this respect the study of hamster lung fibroblasts discussed earlier seems to be quite interesting (Paris and Pouyssegur 1983). The Lineweaver-Burk plot for interaction between  $\text{Na}^+$  and  $\text{H}^+$  ions

given in this work can be referred to as the type shown in Fig. 1a. It is, therefore possible to suggest the presence of a competitive  $\text{Na}^+/\text{H}^+$  antiporter in lung fibroblasts. Nevertheless, the inhibiting effect of amiloride at different concentrations of  $\text{Na}^+$  and  $\text{H}^+$  ions is also shown here (Figs. 4a and 4b). A direct competition between  $\text{Na}^+$  and amiloride (see Fig. 4a) as well as a more complicated interaction with protons (see Fig. 4b) are evident since the Lineweaver-Burk plots have no point of intersection on the ordinate.

On the basis of such contradictory properties we propose that the antiporter has different binding sites for  $\text{Na}^+$  and  $\text{H}^+$  though it is impossible for both ions to be bound simultaneously (otherwise no graphs of 1a type could be obtained). Amiloride competes with  $\text{Na}^+$  for a binding site but the nature of their binding is different since amiloride binding does not prevent protons from binding (see Fig. 4b).

Such a scheme can actually explain a set of experimental data, though one should bear in mind that it is just one of a number of possibilities. Possibly it would be better to consider that  $\text{Na}^+$  and  $\text{H}^+$  ions compete for one and the same site due to the simple competitive kinetics observed. As for amiloride it binds at some other part of the antiporter, causing some changes in its conformation so that  $\text{Na}^+$  binding is inhibited, while protons still retain this ability (see Fig. 9). Such a model would be characterized as shown in Fig. 1a and 4. The same conclusion was made as a result of the study of renal brush border vesicles (Ives et al. 1983), i. e.  $\text{Na}^+$  and  $\text{H}^+$  compete for one and the same site while amiloride is bound elsewhere.

Unlike the antiport model described in this paper the symport model suggests from the very beginning the availability of separate binding sites for  $\text{Na}^+$  and  $\text{OH}^-$ . When analyzing the role of amiloride we introduced a separate binding site for it as well. Due to the stability coefficients ( $\lambda$ ) of complexes it is possible to consider a number of variants including the one with the coinciding sites. For this reason even a simple variant can provide interesting models of symport.

The idea of the existence of two different binding sites, representing transport and control (modifying) sites, has been cited in the literature. Amiloride as well as pH are capable of performing control functions. Generally speaking pH produced a strong effect on the functioning of enzymes (including these mediating transfer). In work on the exchange in renal microvillus membrane vesicles (Aronson et al. 1982) the concept of the control role of pH in  $\text{Na}^+ - \text{H}^+$  exchanger functioning was initially proposed. The authors disclosed a strong effect of pH on the exchange kinetics and it was accounted for by higher (than that of the first order) dependence of the process on  $[\text{H}^+]_i$  or by the presence of control site on the cytoplasmic side of the membrane.

The latter seems to be more probable and it was also supported by the data

on  $\text{Na}^+ - \text{H}^+$  exchange function in rat thymus lymphocytes during  $\text{Na}^+/\text{Na}^+$  exchange (Grinstein et al. 1984). Figs. 6d and 8d show that  $\text{Na}^+/\text{Na}^+$  exchange increases at higher pH in both types of coupled transport. It was also shown that the exchange had stopped at pH 7.0. This fact was interpreted as a pH<sub>i</sub> effect on some control center.

Unfortunately in literature there are no systematic data on  $\text{Na}^+/\text{Na}^+$  exchange which could be helpful in studying the control site effect. The effect is presumably exhibited by enzyme inactivation during  $\text{H}^+$  adsorption ( $\text{OH}^-$  desorption). It can be included in the above considered kinetic schemes if the carrier motility ( $v$ ) is assumed to be correspondingly dependent on pH.

Another control site affected by amiloride is believed to be located on the outer side of the membrane. Some authors (Paris and Pouyssegur 1983) consider it to be identical to the  $\text{Na}^+$  transport site while the others (Ives et al. 1983) have proposed that it is an independent control centre. Nature can possibly provide examples of both variants. Only the direct structural and functional study of proteins involved in exchange transport can provide the final solution to the problems in question.

**Acknowledgement.** I wish to thank Prof. Yu. A. Chizmadzhev and Prof. V. P. Skulachev (Corresponding Member of USSR Academy of Sciences) for valuable and constructive critical discussion of this work.

## References

- Aronson P. S., Nee J., Suhm M. A. (1982): Modifier role of internal  $\text{H}^+$  in activating the  $\text{Na}^+/\text{H}^+$  exchanger in renal microvillus membrane vesicles. *Nature (London)* **299**, 161—163
- Benos D. J. (1982): Amiloride: a molecular probe of sodium transport in tissues and cells. *Amer. J. Physiol.* **242**, C131—C145
- Cala P. M. (1980): Volume regulation of *Amphiuma* red blood cells. The membrane potential and its implications regarding the nature of the ion-flux pathways. *J. Gen. Physiol.* **76**, 683—708
- Drachev A. L., Markin V. S., Skulachev V. P. (1985):  $\Delta\mu\text{H}$ -buffering by  $\text{Na}^+$  and  $\text{K}^+$  gradients in bacteria. Model and experimental systems. *Biochim. Biophys. Acta* **811**, 195—213
- Grinstein S., Cohen S., Rothstein A. (1984): Cytoplasmic pH regulation in thymic lymphocytes by an amiloride — sensitive  $\text{Na}^+/\text{H}^+$  antiport. *J. Gen. Physiol.* **83**, 341—369
- Grinstein S., Goetz J. D., Rothstein A. (1984):  $^{22}\text{Na}^+$  fluxes in thymic lymphocytes. II. Amiloride-sensitive  $\text{Na}^+/\text{H}^+$  exchange pathway; reversibility of transport and asymmetry of the modifier site. *J. Gen. Physiol.* **84**, 585—600
- Heinz E., Geck P., Wilbrandt W. (1972): Coupling in secondary active transport. Activation of transport by co-transport and/or countertransport with the fluxes of other solutes. *Biochim. Biophys. Acta* **255**, 442—461
- Ives H. E., Yee V. J., Warnock D. J. (1983): Mixed type inhibition of the renal  $\text{Na}^+/\text{H}^+$  antiporter by  $\text{Li}^+$  and amiloride. Evidence for a modifier site. *J. Biol. Chem.* **258**, 9710—9716
- Jung D., Schwarz W., Passow H. (1984): Sodium-alanine co-transport in oocytes of *Xenopus laevis*:

- correlation of alanine and sodium fluxes with potential and current changes. *J. Membrane Biol.* **78**, 29—34
- Kinsella J. L., Aronson P. S. (1980): Properties of the  $\text{Na}^+ - \text{H}^+$  exchanger in renal microvillus membrane vesicles. *Amer. J. Physiol.* **238**, F461—F469
- Kinsella J. L., Aronson P. S. (1981): Amiloride inhibition of the  $\text{Na}^+ - \text{H}^+$  exchanger in renal microvillus membrane vesicles. *Amer. J. Physiol.* **241**, F374—F379
- Krulwich T. A. (1983):  $\text{Na}^+/\text{H}^+$  antiporters. *Biochim. Biophys. Acta* **726**, 245—264
- Liberman E. A., Mokhova E. I., Skulachev V. P., Topaly V. P. (1968): Action of oxidative phosphorylation uncouplers on bimolecular phospholipid membranes. *Biofizika*, **13**, 188—193 (in Russian)
- Markin V. S., Chizmadzhev Yu. A. (1974): Induced Ion Transport. Nauka, Moscow (in Russian)
- Martin W. H., Beavis A. D., Garlid K. D. (1984): Identification of an 82,000-dalton protein responsible for  $\text{K}^+/\text{H}^+$  antiport in rat liver mitochondria. *J. Biol. Chem.* **259**, 2062—2065
- Nuccitelli R., Deamer D. W. (1982): Intracellular pH. Alan R. Liss, Inc., New York
- Paris S., Pouyssegur J. (1983): Biochemical characterization of the amiloride-sensitive  $\text{Na}/\text{H}$  antiport in Chinese hamster lung fibroblasts. *J. Biol. Chem.* **258**, 3503—3508
- Rindler M. J., Saier M. H. (1981): Evidence for  $\text{Na}^+/\text{H}^+$  antiport in cultured dog kidney cells. *J. Biol. Chem.*, **256**, 10820—10825
- Saktor B. (1977): Transport in membrane vesicles isolated from the mammalian kidney and intestine. *Curr. Top. Bioenerg.* **6**, 39—81
- Segel J. H. (1975): *Enzyme Kinetics*. J. Wiley and Sons, New York
- Skulachev V. P. (1978): Membrane-linked energy buffering as the biological function of the  $\text{Na}^+/\text{K}^+$  gradient. *FEBS Lett.* **87**, 171—179
- Vigne P., Frelin C., Cragoe E. J., Lazdunski M., (1983): Ethylisopropyl-amiloride: a new and highly potent derivative of amiloride for the inhibition of the  $\text{Na}^+/\text{H}^+$  exchange system in various cell types. *Biochem. Biophys. Res. Commun.* **116**, 86—90
- Vigne P., Frelin C., Lazdunski M. (1982): The amiloride-sensitive  $\text{Na}^+/\text{H}^+$  exchange system in skeletal muscle cells in culture. *J. Biol. Chem.* **257**, 9394—9400
- Weinman S. A., Reuss L. (1982):  $\text{Na}^+ - \text{H}^+$  exchange at the apical membrane of *Necturus* gallbladder. *J. Gen. Physiol.* **80**, 299—321
- Wilbrandt W. (1972): Coupling between simultaneous movements of carrier substrates. *J. Membrane Biol.* **10**, 357—366